

# POST-LINAC BEAM TRANSPORT AND COLLIMATION FOR THE UK'S NEW LIGHT SOURCE PROJECT

D. Angal-Kalinin, J. L. Fernandez-Hernando, F. Jackson, B. Muratori,  
ASTeC/STFC, Daresbury Laboratory, U.K.

## Abstract

The next generation light source for the UK requires transport, collimation and dumping of high power, high quality beams. The accelerated beam must be transported to several different FELs. A design for the post-linac beam collimation, spreader including tomography diagnostics, and beam dumps is presented.

## INTRODUCTION

The New Light Source (NLS) facility for the UK [1] requires an accelerator design to provide 2.25 GeV, 200 pC bunches at a repetition rate of 1 KHz in the baseline extending to 1 MHz in the upgrade path. The baseline beam power is 450 W and 450 kW in the upgrade. The facility needs to provide beam halo collimation to protect the undulator from demagnetisation. The beam spreader distributes the electron bunches to three FEL beam lines in the baseline with the possibility to implement further FEL beam lines. An additional branch of the spreader includes beam tomography section to characterise the full beam phase space. After the undulator in each FEL Line, the electron beam is sent to the beam dump. Two beam dump designs, one as a solid graphite block and one with a conical entrance are proposed.

## BEAM COLLIMATION

A collimation system is necessary in NLS to deal with the beam halo which may be generated by dark current in the injector and in the accelerating modules, scattering from residual gas particles, off-energy beam tails caused by coherent synchrotron radiation (CSR) in the bunch compressors. If not collimated, this beam halo can demagnetize the undulator magnet, cause Bremsstrahlung co-axial with the photon beam lines and can activate the components of the facility. Collimating the beam halo as near as possible to the various sources is preferred as this reduces the overall radiation levels in the machine.

Research at FLASH has concluded that without halo collimation significant demagnetization of the undulator magnets can occur very quickly for kW beam powers [2]. The post linac collimation scheme for NLS is dictated by the requirement of protecting the undulators.

### Collimation Strategy and Design Requirements

The post-linac collimation design strategy removes the beam halo particles in dedicated transverse and energy collimation sections. The collimation schemes used or proposed at other facilities such as FLASH, X-FEL, LCLS and BESSY FEL have been reviewed. The collimation scheme devised for the BESSY FEL design [3] has been adopted for NLS as it is simple and adequate.

A single dedicated collimation section has been proposed immediately after the Linac but before the spreader. Figure 1 shows the optical functions of the collimation section. Transverse collimation is achieved using two betatron collimators separated by  $\pi/2$  phase advance in each transverse plane. A dog-leg located after the betatron collimation section contains energy collimators at either or both high dispersion points. The betatron collimator aperture is determined by the undulator gaps and beam optics and is provisionally expected to be 4 mm (half-gap). The energy collimators must shadow the energy acceptance of the undulators which is approximately  $\pm 5\%$ , translating to a collimator gap of 4 mm (half-gap). These apertures should ensure passive undulator protection for arbitrary beam halo distributions.

Effects of magnet position and field errors, jitter and their effect on collimation need to be studied. Machine failure scenarios will also be investigated; additional protection collimators may be required after the spreader. The wakefields of the collimators may degrade bunch properties. Reliable theoretical estimates and simulations of collimator wake fields have not yet been established for the NLS beam parameters. However, practical experience with TTF2/FLASH [4] shows that it is possible to operate a FEL with a similar collimation system and similar beam parameters without serious wakefield effects.

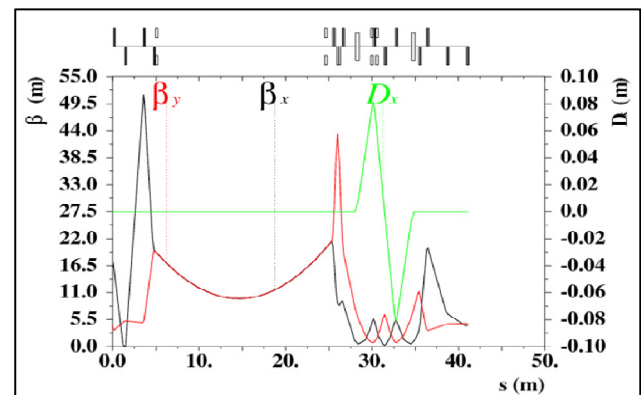


Figure 1: Optics of the post-linac collimation section. Two betatron collimators are separated by  $\pi/2$  phase advance and collimators are located at the high dispersion point in the dog-leg to collimate in the longitudinal plane.

## BEAM SPREADER

The post-linac collimated beam passes through the beam spreader to deliver the beam to different FEL lines. The NLS spreader design needs to switch the electron beam to three FEL beam lines in the baseline 1 KHz operation with the possibility of diverting all the bunches

to any one FEL at a time. The design also needs to be compatible with future increases in repetition rate and the possible addition of extra FEL lines.

The design options for spreading the beam are based on either RF separation or fast kickers [5][6]. The scheme

based on fast kickers, similar to the LBNL design [7] has been chosen for the NLS due to its capacity to increase the number of FEL beam lines without major changes in the facility layout and also to allow full flexibility in the repetition rate for individual FEL beam lines.

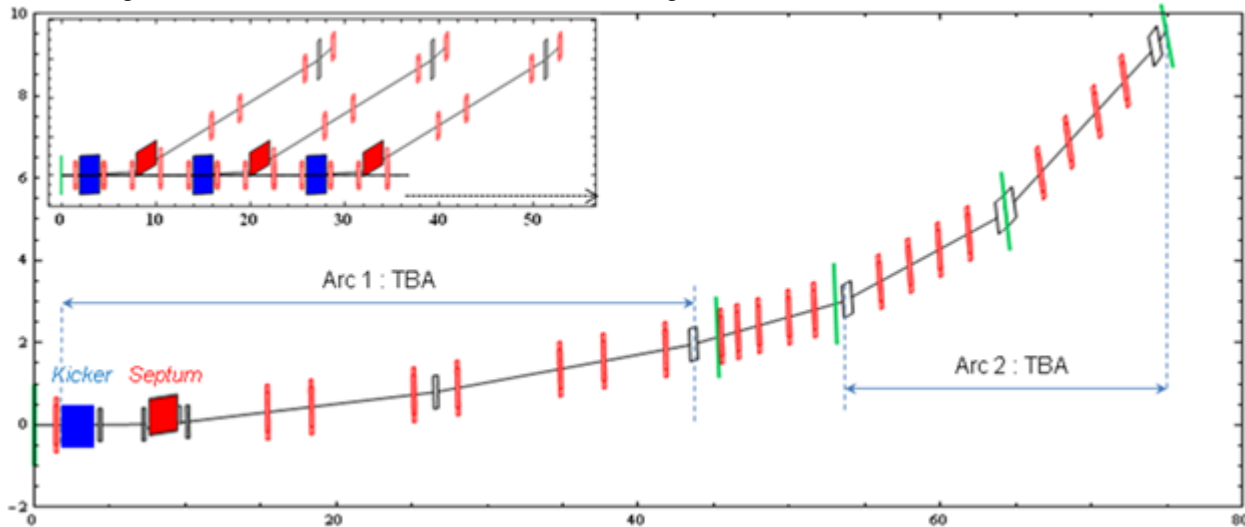


Figure 2: Layout of NLS spreader design based on the LBNL design [9] with fast kicker and septum. The inset on the left hand corner shows start of different FEL beam lines and the figure shows details of the complete lattice for one spreader line.

### Spreader Design

The spreader consists of a long FODO section with a series of extraction points for various FEL lines. Each extraction section consists of two Triple Bend Achromat (TBA) arcs, where the kicker and the septum replace the first dipole of the first TBA arc. A 2 meter long kicker placed between the first F and D quadrupole provides a kick of 3 mrad. The septum kicks the beam by 27 mrad. The beam passes off-axis in the D quadrupole immediately after the kicker and through the F quadrupole before the septum. The off-axis beam passing through the D quadrupole after the septum gives an additional bend of 17 mrad, thereby reducing the required strength of the septum magnet. The beam is finally separated from the incoming beam after the D magnet after the septum. Bunches which are not diverted to this particular FEL line continue to pass on-axis through the FODO. The first TBA arc is then completed with two additional dipoles and seven quadrupoles. This section is followed by matching quadrupoles to match the beam into the second TBA arc. The NLS beam spreader optics is shown in Figure 3. The optics has been optimized to be achromatic and isochronous within each arc. Emittance increase and microbunching may occur due to CSR from passing very short bunches through the spreader dipoles [8]. Further optimization of the overall  $R_{56}$  in the TBA arcs including its maximum excursion within the arcs. To divert all bunches to any single FEL beam line, it is proposed to include a DC dipole magnet at the location of each kicker. The technology of the kicker and septum and

the implications for the jitter in transverse position and beam arrival time will need further investigation.

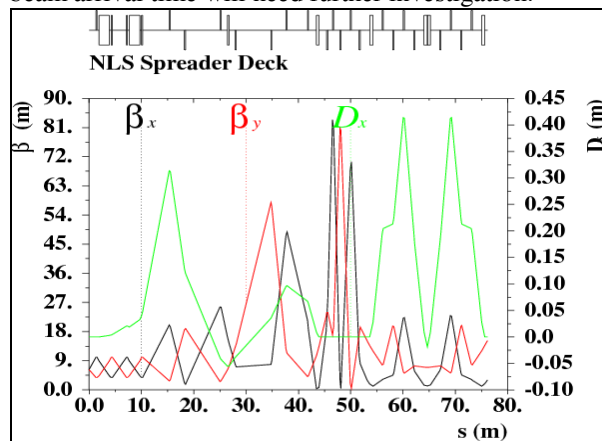


Figure 3: Optics of NLS spreader design including FODO, kicker, septum and TBA arcs.

### TOMOGRAPHY BEAM DIAGNOSTICS

The proposed tomography beam diagnostics section in one of the spreader branches will fully characterize the beam in 6D phase space, which will provide knowledge of projected and slice transverse emittances, longitudinal bunch profile, energy spread, and (by using a spectrometer dipole) slice energy spread. The tomography section is located in the first branch of the beam spreader. This location has several advantages; the measured beam characteristics include the effect of the beam spreader; diagnostics can be performed ‘on-line’ by deflecting

occasional bunches into the branch line and the branch can be used as a commissioning/tuning line without having to send the beam through the undulators. Some additional measurements may also be included in each FEL branch which will complement the dedicated measurements in this branch and highlight the differences, if any.

### Design Details

The tomography diagnostics section consists of a FODO lattice with four screens providing  $45^\circ$  phase advance per screen [9][10] and is preceded by four matching quadrupoles to match to the FODO and two deflecting cavities (one for each transverse plane). The deflecting cavities operate in TEM<sub>110</sub> mode at zero crossing, which allows streaking of the bunch to obtain information on bunch length and slice emittance using one or more tomography screens. For effectiveness of the streak, the beam size at the location of the deflecting cavities needs to be reasonably large and the phase advance between the centre of the cavities and the first screen needs to be an odd integer multiple of  $\pi/2$  or as close as possible to it. Four quadrupoles preceding the deflecting cavities are used to increase the beam sizes at the deflecting cavities. Depending on the direction of the streak, the head of the bunch is deflected downwards whereas the tail of a bunch is deflected upwards. Measurements *without* streak give the projected transverse profiles and emittances, whereas measurements *with* streak measure the slice emittances and the bunch length. This is more important since the effects of space charge and CSR vary along the bunch, and so only the slice emittances give the precise information about the part of the bunch which takes part in the lasing process.

The complete layout of the tomography section is shown in Figure 4. Measurement of the slice energy spread is also a possibility and will need a spectrometer dipole to be included in the diagnostic line.

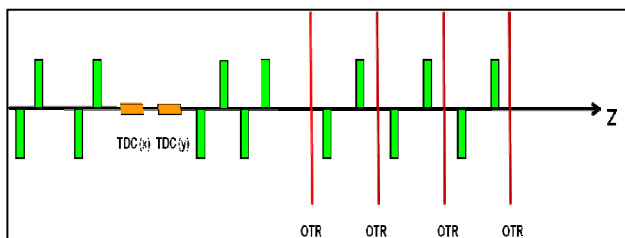


Figure 4: Possible layout of the tomography beam diagnostics line. TDC(x), TDC(y) are the Transverse Deflecting Cavities and OTR is the screen/wire location.

## BEAM DUMPS

The electron beam needs to be dumped after passing through the tomography section in the first branch of the beam spreader as well as after the undulator section in each FEL line.

In the worse case of the full repetition rate, each beam dump has to absorb a power of  $\sim 450$  W when operating at the baseline frequency of 1 kHz and  $\sim 450$  kW when the frequency increases up to 1 MHz. The design requirements for both baseline and upgrade power levels need to be considered to understand the implications on the facility layout.

A solid dump as proposed for the CEBAF tuning line [11] or for X-FEL [12] can be considered for NLS. The beam power is entirely contained in metal in such a dump, minimising the problems associated with radioactive water handling. The beam dump designs require beam rastering when the beam sizes are small.

### Design Options

A solid beam dump with a graphite core is being studied as an initial option for both the baseline and the upgrade frequency case. A water beam dump may be necessary when upgrading to a higher frequency if the heat deposited in the solid beam dump would exceed the fracture or melting limits.

For the initial study of energy deposition in the dump an arbitrary but realistic radial RMS beam size,  $\sigma_r$ , of 2 mm is used in the FLUKA [13][14] simulations. Two different models of a solid dump have been simulated: a regular graphite 1 m long cylinder with a diameter of 1 m, and a graphite cylinder of the same dimensions but adding an entrance cone into the bulk with a base radius of 6 mm. Figure 5 and Figure 6 show the results for the energy deposition in both cases and it can be seen that the entrance cone distributes the beam's energy more efficiently along the length of the cone and the dump, resulting in energy densities that are an order of magnitude smaller. The peak temperature in both cases is the same. Table 1 summarizes the peaks of temperature for both the conical entrance and simple block dumps for the baseline and upgraded frequency. The heating rate does not consider any effects of heat diffusion and cooling. The last column shows the results for a much larger incident beam size. It can be seen that the beam size has a major impact on the deposited energy density in the material and so rastering of beam position would allow simpler cooling or heat extraction solutions. A circular beam sweep, as studied in similar beam dumps [15], is an option that will most likely be used for the design of the NLS beam dump.

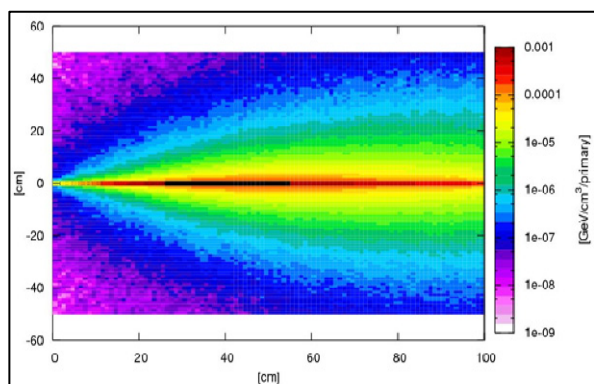


Figure 5: Energy density deposited per primary particle in a graphite beam dump with conical entrance.

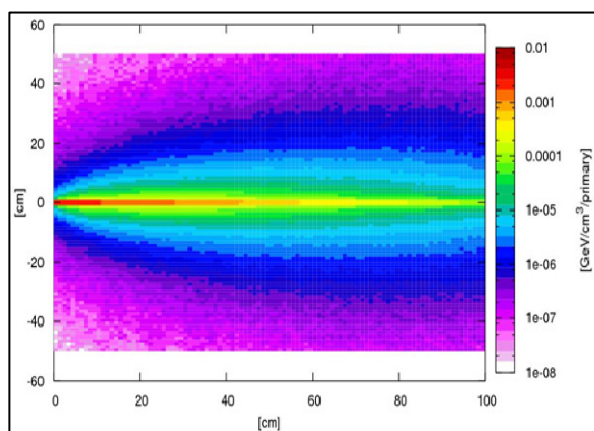


Figure 6: Energy density deposited per primary particle in a simple graphite block.

Table 1: Peak rate of temperature increase for the conical entrance and simple block dump cases.

Beam power (rep. rate)	Beam size 2 mm, conical entrance.	Beam size 2 mm, simple block.	Beam size 2 cm, conical entrance.
450 W (1 kHz)	0.0025 K/bunch, 2.5 K/second	0.0025 K/bunch, 2.5 K/second	0.00004 K/bunch, 0.04 K/second
450 kW (1MHz)	0.0025 K/bunch, 2500 K/second	0.0025 K/bunch, 2500 K/second	0.00004 K/bunch, 40 K/second

### ACKNOWLEDGEMENTS

The authors thank T. Kamps (HZB) for providing the BESSY FEL lattice design for the collimation optics and J. Corlett (LBNL) for useful discussions regarding the LBNL beam spreader design.

### REFERENCES

- [1] R. Bartolini, "Optimisation of a Single-Pass Superconducting Linac as a FEL driver for the NLS Project." These proceedings.
- [2] H. Schlarb, "Collimation System for the VUV Free-Electron Laser at the TESLA Test Facility." PhD Thesis, University of Hamburg, 2001
- [3] T. Kamps, "Collimation System for the BESSY FEL". FEL 2004, Trieste, Italy
- [4] J. Rossbach, "Review of DESY FEL activities." EPAC 08, Genoa, Italy.
- [5] D. R. Douglas, "Design Considerations for Implementing Alternative RF Separator Schemes," CEBAF-TN-91-072, 1991
- [6] R. Brinkmann, "Some Considerations on X-FEL Beam Distribution", DESY internal presentation.
- [7] A. A. Zholents et al "Design of the Electron Beam Switchyard for an array of Free Electron Lasers" CBP Tech Note 401, 2009
- [8] M. Venturini, A. Zholents, "Modeling Microbunching from shot noise using Vlasov Solvers," NIM A, **593**, 53-56, 2008
- [9] F Löhl, "Measurements of the Transverse Emittance at the VUV-FEL", Diploma Thesis, Hamburg, DESY-THESIS 2005-014 and TESLA-FEL 2005-03, 2005
- [10] KHonkavaara K. and Löhl F., Personal Communication. 2005
- [11] Wiseman M. et al, High Power Electron Beam Dumps at CEBAF, PAC97, Vancouver, Canada
- [12] Maslov M., Schmitz M., Sytchev V., Layout Considerations on the 25GeV/300kW Beam Dump of the XFEL Project, DESY, TESLA-FEL, 2006-05
- [13] Fassò A., Ferrari A., Sala P.R., Electron-photon transport in FLUKA: status, Proceedings of the MonteCarlo 2000 Conference, Lisbon, October 23--26 2000, A.Kling, F.Barao, M.Nakagawa, L.Tavora, P.Vaz - eds., Springer-Verlag Berlin, p.159-164, 2001
- [14] Fassò A., Ferrari A., Ranft J., Sala P.R., FLUKA: Status and Prospective for Hadronic Applications, Proceedings of the MonteCarlo 2000 Conference, Lisbon, October 23-26 2000, A.Kling, F.Barao, M.Nakagawa, L.Tavora, P.Vaz - eds. , Springer-Verlag Berlin, p.955-960 (2001).
- [15] Bialowons W., Maslov M., Schmitz M., Sytchev V., Concept of the High Power e<sup>±</sup> Beam Dumps for TESLA, DESY, February 2001, TESLA Report 2001-04